An Improved Temperature Function for Modeling Crop Residue Decomposition

H. H. Schomberg, G. R. Foster, J. L. Steiner, D. E. Stott

Abstract. *Models like the Revised Universal Soil Loss Equation (RUSLE) and Revised Wind Erosion Equation (RWEQ) that estimate erosion potential need good estimates of crop residue decomposition to evaluate changes in soil surface cover. Decomposition is modeled based on climate and residue chemical characteristics as controlling factors. Crop–specific decomposition coefficients account for differences in the chemical and physical properties of the residues. Temperature and water functions relate climatic conditions in the field to optimum conditions. The models use a scaled temperature function (TF) to relate monthly temperature to relative biological activity. The half–month time steps and monthly data used in RUSLE and RWEQ result in the loss of temporal information about temperature effects. Use of average temperature or maximum and minimum temperatures to estimate TF were compared with TF estimated as the integral from maximum to minimum for monthly or daily data. The numerically integrated approach appeared to be more robust and was theoretically more appealing than the two original approaches. However, because RUSLE and RWEQ have been developed for users with limited computer resources, the integrated function was not considered appropriate. A system of equations for calculating TF on a monthly basis was developed that captured the dynamic effect of daily temperatures but required less computation time than the integrated method. Comparison to the original approach in RUSLE for estimating decomposition of wheat residues at several locations in the U.S. indicates significant improvement in model performance. This system of equations should improve decomposition estimates in monthly time step models and could be applicable to daily time step models and other biological processes.*

Keywords. *Revised Universal Soil Loss Equation, Revised Wind Erosion Equation, Crop residue decomposition.*

The Revised Universal Soil Loss Equation (RUSLE) and the Revised Wind Erosion Equation (RWEQ) are used by government agencies, soil erosion specialists, and researchers to predict soil management effects on potential soil erosion from water and wind, respectively. Erosion potential is determined from climatic conditions, soil erodibility, and land management (Foster, 1991; USDA, 1996; Fryrear et al., 2000). These models underwent significant improvements during the late 1990s through development of new relationships based on modern erosion theory and new data. Because of the empirical approaches used in RUSLE and RWEQ, half–month time steps are used to capture seasonality of erosion events and identify critical soil, management, and climate interactions important for reducing erosion potential. In addition, the models are designed for users with limited computer resources and to be relatively easy to learn and quick to use.

An important management factor affecting soil erosion is keeping crop residues on the surface to reduce raindrop impact, slow runoff, increase infiltration, and decrease surface wind speed. Emphasis on crop residue management to meet soil conservation goals has increased the need to accurately reflect the decomposition process in resource planning software. As crop residues decompose, soil protection diminishes. Crop residue decomposition is generally considered to be controlled by substrate quality and availability (Meentemeyer, 1978; Parr and Papendick, 1978; Aber and Melillo, 1982; Reinertsen et al., 1984; and others) and the climatic factors of temperature and water (Stott et al., 1986; Roper, 1985). Laboratory studies indicate that water and temperature have a greater effect during early stages of decomposition, when easily utilizable compounds are readily available to microorganisms (Stott et al., 1986; Roper, 1985). Greater fluctuations in water and temperature, along with reduced nutrient availability, adversely affect microbes colonizing surface residue, thus slowing decomposition, compared with incorporated crop residues (Brown and Dickey, 1970; Douglas et al., 1980).

Water and temperature relationships must be evaluated under a range of field conditions to determine their applicability to long–term prediction. Different approaches in estimating temperature indices were identified as contributing to the disagreement in crop residue decomposition estimation between RUSLE and RWEQ (Schomberg and Steiner, 1997), but a clear indication of the "best" approach for estimating temperature effects was not determined.

Article was submitted for review in August 2000; approved for publication by the Soil & Water Division of ASAE in August 2000.

The authors are **Harry H. Schomberg,** Ecologist, USDA–ARS, J. Phil Campbell Sr. Natural Resource Conservation Center, Watkinsville, Georgia; **George R. Foster, ASAE Fellow Engineer,** Agricultural Engineer, retired (collaborator), USDA–ARS National Sedimentation Laboratory, Oxford, Mississippi; **Jean L. Steiner,** Soil Scientist, USDA–ARS Grazinglands Research Laboratory, El Reno, Oklahoma; and **Diane E. Stott,** Soil Scientist, USDA–ARS National Soil Erosion Laboratory, West Lafayette, Indiana. **Corresponding author:** Harry H. Schomberg, USDA–ARS, J. Phil Campbell Sr. Natural Resource Conservation Center, 1420 Experiment Station Rd., Watkinsville, GA 30677–2373; phone 706–769–5631, ext. 222; fax: 706–769–8962; e–mail: hhs1@arches.uga.edu.

Temperature effects on biological processes are best modeled with data that reflect fluctuations relevant to the process being modeled. Data with greater resolution than might be used in actual modeling of a process can be helpful in developing functions that more closely simulate temperature effects. Limitations to using high–resolution data for running models include lack of appropriate data, long computation times, and a desire to keep the model as simple as possible. Temperature effects have been modeled with functions that simulate daily, monthly, or even yearly mean temperatures, or with an interpolated time course of these data (Lischke et al., 1997). Depending on the time step and sensitivity of the process, each of these approaches results in loss of information about temperature variability, particularly diel variation. Processes that respond to temperature in a nonlinear manner are more sensitive to the type of data used. Overcoming the conflict between precision and manageability requires methods to calculate physiological time as precisely as needed using information from available input data. The methods should be able to express temperature effects from smaller to larger time scales (Lischke et al., 1997).

The objective of this study was to develop an improved approach for calculating a temperature function (TF) over a range of environmental conditions for RUSLE and RWEQ. In addition, we wanted to improve commonality and agreement with the Water Erosion Prediction Project (Stott et al., 1995) and the Wind Erosion Prediction System (Steiner et al., 1995) models, which are based on a daily time step. We compared the currently used approach of calculating TF from maximum and minimum temperature (RWEQ) and from average temperatures (RUSLE) with an integrated approach using monthly and daily data simulated for 18 locations in the U.S. (table 1). Using results from the integrated approach, we developed a system for calculating TF using monthly maximum and minimum temperatures that agreed closely with estimates from daily maximum and minimum temperatures. In addition, the new approach was developed within the concept of minimizing run times and using simple approaches within the models. Development of the equations is presented so that others may consider the approach in similar models or where temperature functions need to be adapted from hourly or daily time step models to longer time steps.

Table 1. Locations used for generation of temperature data with the CLIGEN weather simulator, and simulated average January, July, and yearly temperatures and the difference between maximum and minimum temperatures for January and July (years = 30).

	January		July		Year
Location	Avg	$t_{max}–t_{min}$	Avg	$t_{max}–t_{min}$	(Avg)
St. Paul, Minn.	–10.9	10.5	22.5	11.2	6.7
Portland Maine	–5.8	10.6	19.9	11.1	7.2
Pierre, S.D.	–9.2	12.1	23.7	15.4	7.9
Moscow, Idaho	–2.3	7.6	18.6	19	8.3
Scotts Bluff, Neb.	–3.2	13.1	23	16.7	9.2
Pomeroy, Wash.	–0.7	9.6	21.2	18.6	10.3
Tooele, Utah	–2.1	10.5	23.9	14	10.3
Jefferson City, Mo.	–1.5	12.5	25.4	13.8	12.5
Baltimore, Md.	0.3	10	24.9	11.4	12.7
Vega, Texas	1.3	15.7	24.9	15.4	13.1
Holly Springs, Miss.	2.4	11.9	25.8	12	14.7
Siloam, Ga.	6.3	12.1	26.3	12.2	16.8
Button Willow, Cal.	7.1	12.1	27.3	18.4	17.2
Pascagoula, Miss.	9.7	10.9	27.8	9.1	19.7
Tucson, Ariz.	10.7	14.2	29.9	14.3	20.1
Homestead, Fla.	18.4	12.8	27	10.7	23.2
Yuma, Ariz.	13.6	13.6	34	14.8	23.4
Death Valley, Cal.	11.5	14.6	38.1	15.4	24.6

MODEL DESCRIPTION

In RUSLE and RWEQ, the mass loss of surface and buried residues is predicted with the following exponential decay function:

$$Mass_{remaining} = Mass_{initial} \times e^{(-k \times time)} \tag{1}$$

where

$Mass_{remaining}$ = estimated from initial mass
$-k$ = crop–specific decomposition coefficient that accounts for differences in chemical and physical properties of residues
$time$ = estimated for the period based on a decomposition day approach, much like growing degree days for crop growth models.

Decomposition days for a period are estimated from scaled climatic functions for water and temperature. Under non–water limiting conditions, temperature is the controlling climatic factor for residue decomposition. A temperature function (TF) used by Stroo et al. (1989) to model wheat (*Triticum aestivum* L.) residue decomposition was adopted for use in RUSLE and RWEQ. The same equation is used in the Water Erosion Prediction Project (Stott et al., 1995) and the Wind Erosion Prediction System (Steiner et al., 1995), which enhances commonality among the models. Biological activity at field temperatures is related to activity under optimal conditions using a relative scale of 0 to 1. When temperatures are less than ideal, decomposition is reduced to a fraction of the optimal rate. The function is:

$$\mathrm{TF} = \frac{2(t+A)^2 (t_{opt}+A)^2 - (t+A)^4}{(t_{opt}+A)^4} \tag{2}$$

where

t = air temperature for the current period
t_{opt} = optimum air temperature for decomposition, and determines where TF = 1
A = coefficient indicating the lower limit for microbial activity, and the point where TF = 0.

RUSLE and RWEQ use $A = 0°$ C and $t_{opt} = 32°$ C, which is slightly different from the values used by Stroo et al. (1989). Applying these values to equation 2 results in:

$$\mathrm{TF} = \frac{2 \times 32^2 t^2 - t^4}{32^4} \tag{3}$$

Currently, RWEQ calculates TF from maximum and minimum half–month (14, 15, or 16 d) temperatures and then averages to obtain a TF value for the period, while RUSLE uses average half–month temperature to calculate a TF value. These two approaches result in significantly different TF values depending on the numeric difference between the maximum and minimum temperatures and due to the nonlinear nature of equation 2 (fig. 1) (Schomberg and Steiner, 1997).

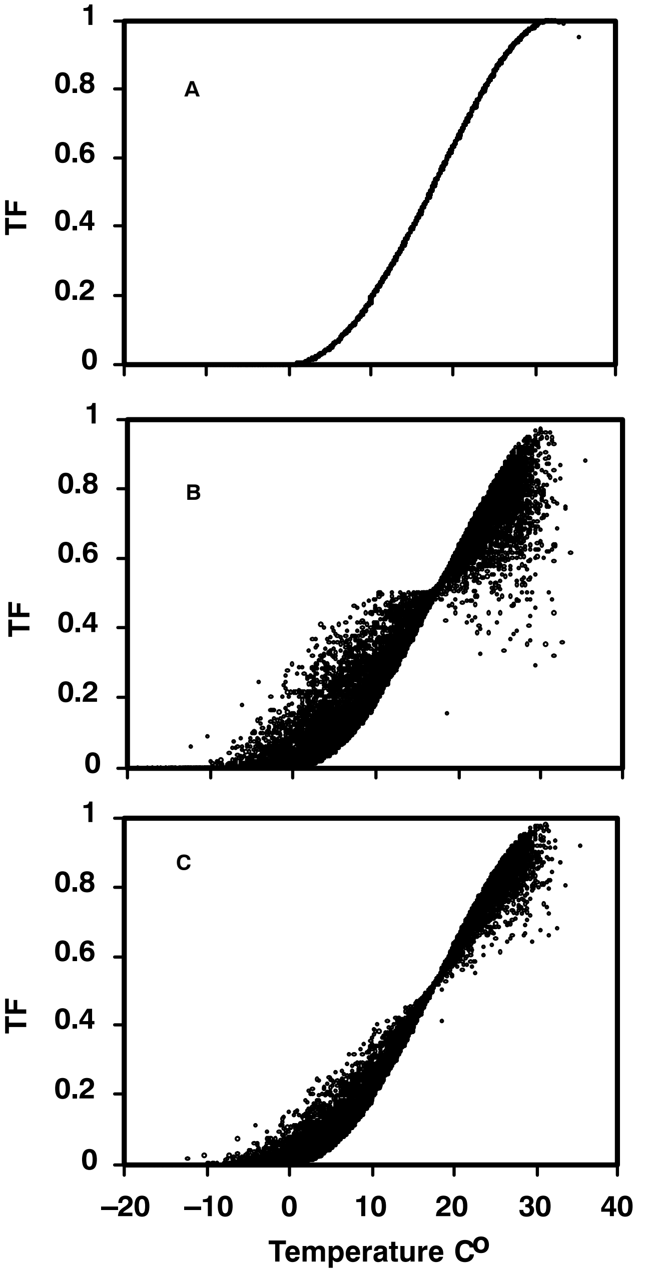

Figure 1. Daily values of the temperature function (TF) for Jefferson City, Missouri, estimated from (a) daily average temperature, (b) daily maximum and minimum temperatures, and (c) hourly temperatures that were integrated into a daily value.

Methods

Climate Simulations

Thirty years of daily maximum and minimum temperatures were simulated with CLIGEN version 5.107 (USDA–ARS, 2001; Nicks et al., 1995) for 18 locations across the U.S. (table 1). Data were averaged to produce daily and monthly maximum, minimum, and average temperatures, which were then used to calculate TF for each day and month. A 24–hr integrated value of daily TF was calculated for each location assuming daily temperatures varied between maximum and minimum temperatures according to a sine function, as follows:

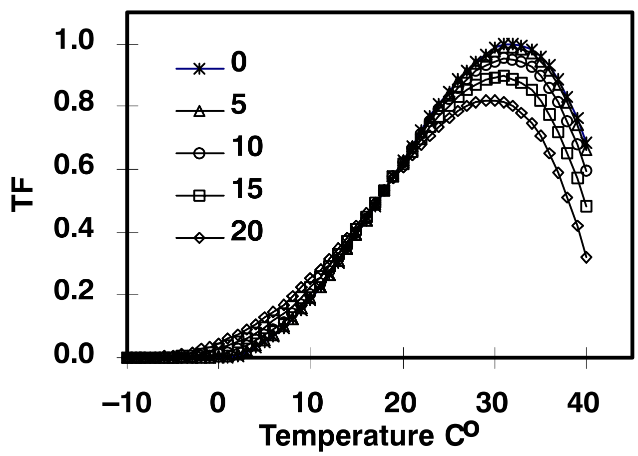

Figure 2. Graphical representation of the TF database developed for a range of maximum and minimum temperatures differing by 0° C, 5° C, 10° C 15° C, and 20° C using the integrated temperature function.

$$t_h = \frac{t_{max} - t_{min}}{2} \times \sin\left(2 \times \frac{h}{24} \times \Pi\right) + \frac{t_{max} + t_{min}}{2} \qquad (4)$$

where

t_h = temperature for each hour (h)
t_{max} = maximum daily temperature
t_{min} = minimum daily temperature.

Next, equation 4 was substituted into equation 3 and numerically integrated to estimate a TF value for each day ($TF_{integrated}$). Data from CLIGEN (above) were used to calculate $TF_{integrated}$ for each location in table 1. Monthly values of $TF_{integrated}$ were calculated from monthly maximum and minimum values using a time step of 30 instead of 24. Monthly and daily values of TF and $TF_{integrated}$ were used to evaluate differences among the methods. Regression of TF values against $TF_{integrated}$ was used to determine the root mean square error (RMSE), correlation coefficient (R^2), and coefficient of variation (CV) (SAS, 1989).

The comparisons indicated that an integrated TF provided a better approach than the two original approaches. Run–time limitations within RUSLE and RWEQ prohibited the use of the integrated approach; therefore, a system of equations was developed to capture the results observed with $TF_{integrated}$ that was consistent with the form of the original temperature function (eq. 3). Equations for the new function (TF2) were derived from $TF_{integrated}$ values calculated from a synthetic data set having a range of temperatures from –20° C to 40° C with maximum and minimum temperature differences of 0° C, 5° C, 10° C, 15° C, and 20° C (fig. 2). Equations developed for four subregions of the original TF equation (eq. 3) were chosen and fit using a minimum of parameters. Coefficients and exponents for equations were determined using ordinary least–square fits with the MODEL procedure of SAS ETS (SAS, 1988).

Validation of Approach

Data on mass loss of wheat residue from published literature were used to compare the original TF approach in RUSLE to the new TF2 approach for estimating decomposition. The same routines will be used in RWEQ and were not included in this comparison. Data were selected from studies in Georgia, Texas, Indiana, and Oregon. Climatic data were obtained from the publication authors. Decomposition in field environments was measured as mass loss between sampling periods for residues on the soil surface in the field. Details of the studies can be found in Douglas et al. (1980), Stott et al. (1990), Ford (1991), Schomberg et al. (1994), Steiner et al. (1994), and Schomberg and Steiner (1997). Comparisons were evaluated by regressing observed versus predicted values and determining the R^2, RMSE, and CV. In addition, agreement between predicted and measured population means and variances were evaluated with a paired t–test for means and an F ratio test of variances. A chi–squared test for lack of fit and an estimate of the accuracy of prediction was determined using the procedures of Freese (1960).

Results and Discussion

Comparison of TF from Maximum–Minimum, Average, and Integrated Temperatures

The three methods of estimating TF produce visually different results for the locations in table 1, as illustrated for Jefferson City, Missouri (fig. 1). The $TF_{integrated}$ values from daily data were more similar to TF values calculated from daily maximum and minimum temperatures than to TF values calculated from average daily temperatures. When compared against $TF_{integrated}$, the RMSEs, R^2, and CVs were 0.11, 0.89, and 25.6, respectively, for TF values from daily maximum and minimum temperatures and 0.15, 0.67, and 64.7, respectively, for TF values from daily average temperatures. Figure 1a demonstrates the limited temperature variability captured when using daily average temperatures. Estimation of TF from daily maximum and minimum temperatures introduces significant variation (fig. 1b) with distinct upper and lower boundaries below and above the inflection point of equation 3. The $TF_{integrated}$ values (fig. 1c) show a tighter distribution near the plot of equation 3 than for TF from daily maximum and minimum temperatures (fig. 1b) and are still restricted by the upper and lower limits of the original temperature function. Conceptually, values from $TF_{integrated}$ should more closely reflect diurnal effects because equation 4 integrates temperatures from maximum to minimum for each 24–hr period. A greater dynamic response for $TF_{integrated}$ values is apparent near the upper and lower range of the scale and is attributable to the magnitude of the difference between maximum and minimum temperatures (near 0 and 1, compare figs. 1a and 1c).

Results comparing the three estimates of TF from monthly data for the 18 locations are similar to the results with daily data (fig. 3). Again, monthly average temperatures produce a smooth plot of equation 3, while temperature variation is present when using maximum and minimum temperatures, especially near 0 and 1, and as TF values decline beyond the maximum TF value (fig. 3). Values of TF from maximum and minimum data more closely agreed with daily $TF_{integrated}$ values than with monthly $TF_{integrated}$ values. Surprisingly, TF values estimated from maximum and minimum data and those from average data compared similarly to monthly $TF_{integrated}$. Plots of residuals for monthly TF estimates indicated larger deviations from $TF_{integrated}$ values below 0.20 and above 0.70, or the upper and lower portion of equation 3, for both maximum and minimum and average data (data not

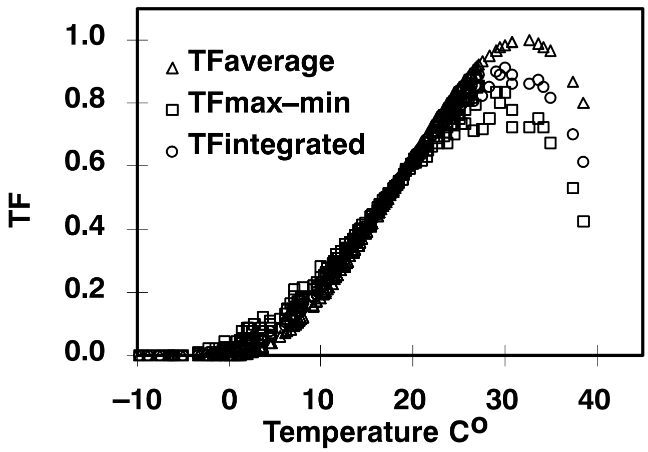

Figure 3. Monthly TF estimates for 18 locations in the U.S. using average temperature ($TF_{average}$), maximum and minimum temperatures ($TF_{max–min}$), and an integrated value determined using temperatures from the maximum to the minimum ($TF_{integrated}$).

presented). The integrated approach should more closely represent temperature effects on residue decomposition, and the greater similarity of results for monthly data reiterates the loss of dynamics due to large time steps. Divergence from $TF_{integrated}$ by values estimated with equation 3 and average or maximum and minimum temperatures appeared to be related to the magnitude of the difference between maximum and minimum temperatures. This was increasingly apparent for values near the upper and lower ends of the function.

Developing a New Method to Calculate TF (TF2)

The integrated approach would eliminate problems of which type of data to use and problems in estimating TF at the upper and lower limits of equation 3. However, the integrated function was not appropriate for RUSLE and RWEQ because of run–time limitations placed on subroutines in the erosion models by the developers and users of these models. A system of equations was developed that was consistent with the original temperature function (eq. 3) and captured the results observed with $TF_{integrated}$. Equations to calculate the new temperature function (TF2) were developed with a synthetic data set and chosen to use a minimum number of parameters based on the monthly maximum and minimum temperatures. Four regions of the original function were identified for equation development:

Region 1: the minimum critical temperature ($t_{critical}$) for biological activity, below which no decomposition occurs.

Region 2: from region 1 to the inflection point ($t_{inflection}$) of equation 3.

Region 3: from the inflection point of equation 3 to the peak temperature (t_{peak}), where TF2 reaches a maximum value.

Region 4: from the maximum TF value to an upper temperature limit (40° C, the upper limit of temperatures from the 18 locations used in the initial analysis).

Equations for regions 2 and 3 define TF2 for most of the temperature range and subsequently were used in developing equations for regions 1 and 4. The defining point between regions 2 and 3 is the inflection point of equation 3, which is determined by taking the second derivative, solving for the temperature where this derivative is zero (18.48° C), and using this value in equation 3 to determine the corresponding TF value (0.556). This point also served as the upper limit of region 2. The $TF_{integrated}$ values calculated for temperatures below 18.5° C were used for fitting a relationship for region 2 (fig. 2) and for defining the lower boundary, which also produces the defining criteria for $t_{critical}$ (region 1). Separations between the lines in figure 2 represent the amplitude between maximum and minimum temperatures. The following equation represents region 2:

$$TF2 = a\left(\frac{t_{average} - t_{critical}}{18.48 - t_{critical}}\right)^{m} \quad (5)$$

where

$t_{average}$ = average monthly temperature
a = upper limit of region 2 (0.556)
m = exponent defining the rate of ascent of the power function.

The relationship for $t_{critical}$ was based on the plotted data (fig. 4), which indicated that the average temperature for the lower limit of microbial activity declined as the difference between maximum and minimum temperatures increased and was described with the following equation (R^2 = 1.0):

$$t_{critical} = 0.5(t_{max} - t_{min}) \quad (6)$$

An equation for m in equation 5 was developed based on the change in TF2 associated with the magnitude of the difference between maximum and minimum temperatures. Data values below the inflection were used with equations 5 and 6 to determine values of m. Plots of m versus the difference between maximum and minimum temperatures indicated a quadratic relationship, as follows (R^2 = 0.99):

$$m = 1.79 + 0.075(t_{max} - t_{min}) - (2.56E{-3})(t_{max} - t_{min})^2 \quad (7)$$

Region 3 of TF2 extends from the inflection point to the optimum temperature for microbial activity. The equation derived to describe this region is:

$$TF2 = TF2_{peak} - b(t_{peak} - t_{average})^{1.71} \quad (8)$$

where

t_{peak} = average monthly temperature at the optimum temperature ($TF2_{peak}$)
b = coefficient dependent on differences between maximum and minimum temperatures.

It was observed from plots of the $TF_{integrated}$ values (fig. 2) that t_{peak} and $TF2_{peak}$ varied with the difference between maximum and minimum temperatures. The data in figure 2 were used to plot this effect (fig. 5) and develop the following equations describing change in TF_{peak} (R^2 = 0.99) and t_{peak} (R^2 = 0.99):

$$t_{peak} = 32 - (6.43E - 3)(t_{max} - t_{min})^{1.98} \quad (9)$$

$$TF_{peak} = 1 - (5.31E - 4)(t_{max} - t_{min})^{1.95} \quad (10)$$

The coefficient b and exponent for equation 8 were determined for equations 9 and 10 by fitting equation 8 to the $TF_{integrated}$ values for region 3. The exponent showed little effect of temperature differences, while the relationship between b and maximum and minimum temperatures (R^2 = 0.98) was described with the following equation:

$$b = 0.0053 - (2.23E - 6)(t_{max} - t_{min})^2 \quad (11)$$

The convergence point between regions 2 and 3 (eqs. 5 and 8) varied due to the size of the difference between maximum and minimum temperatures. Because the convergence point varied from the hypothesized common point a (0.556), a relationship was determined for a in equation 5 based on the difference between maximum and minimum temperatures. This relationship allows equations 5 and 8 to converge at a, thus giving continuous values over regions 2 and 3 (R^2 = 0.96). The equation for a is:

$$a = 0.559 + 6.96E - 4(t_{max} - t_{min}) - (4.01E - 5)(t_{max} - t_{min})^2 \quad (12)$$

For region 4, the following equation was used to describe the decline in TF2 for temperatures above the optimum for microbial activity:

$$TF2 = TF_{peak} - c(t_{average} - t_{peak})^{n} \quad (13)$$

where c is a coefficient, and n is an exponent. This equation has the important properties of TF2 equaling TF_{peak} at the temperature where $t_{average}$ equals t_{peak} and having a zero slope at t_{peak}. The $TF_{integrated}$ values for temperatures above TF_{peak}

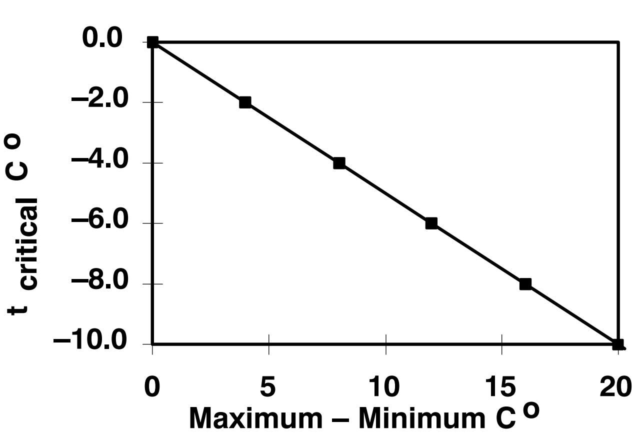

Figure 4. Change in the lower temperature limit for microbial activity ($t_{critical}$) due to the difference between maximum and minimum temperatures.

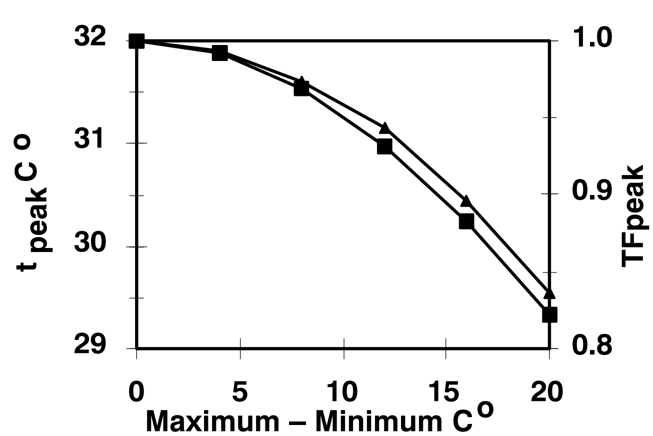

Figure 5. Change in the maximum TF value (TF_{peak}) and the peak temperature (t_{peak}) due to the difference between maximum and minimum temperatures.

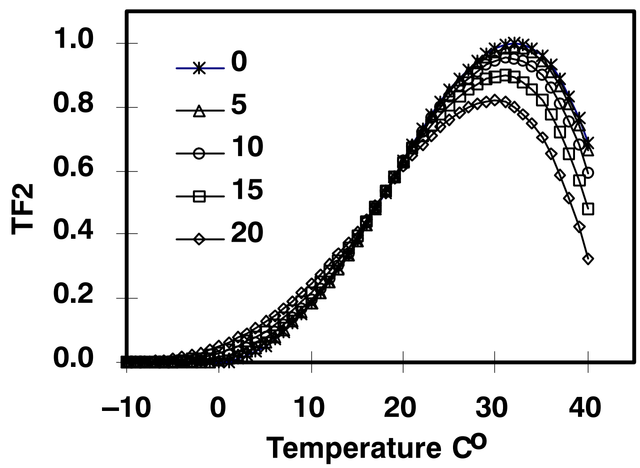

Figure 6. Graphical representation of the new temperature function (TF2) values calculated using the developed system of equations for a range of maximum and minimum temperatures differing by 0° C, 5° C, 10° C, 15° C, and 20° C.

Table 2. Comparison of methods for estimating TF from monthly data to $TF_{integrated}$ estimated using daily or monthly data for the 18 locations in table 1.

	$TF_{integrated}$					
	Daily[a]			Monthly		
Monthly	RMSE[b]	R^2	CV	RMSE	R^2	CV
$TF_{average}$[c]	0.039	0.986	9.22	0.028	0.993	6.77
$TF_{max-min}$[d]	0.023	0.993	5.60	0.028	0.989	6.85
$TF_{integrated}$	0.013	0.998	2.89	—	—	—
TF2[e]	0.017	0.996	4.07	0.017	0.996	4.44

[a] Daily $TF_{integrated}$ values were averaged for each month prior to the analysis.
[b] Root mean square error (RMSE), correlation coefficient (R2), and coefficient of variation (CV).
[c] $TF_{average}$ is calculated from average temperatures for the month.
[d] $TF_{max-min}$ is calculated from monthly maximum and minimum temperatures and then averaged for a single monthly value.
[e] TF2 is calculated from the series of equations using monthly data.

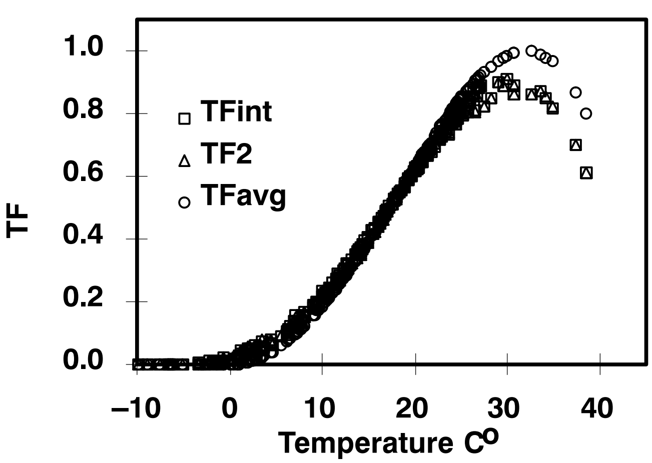

Figure 7. Monthly TF estimates for 18 locations in the U.S. using average temperature ($TF_{average}$), integrated temperatures from the maximum to the minimum ($TF_{integrated}$), and maximum and minimum temperatures using the developed system of equations (TF2).

were used with equation 13 to develop the following equations for c(R^2 = 0.96) and n (R^2 = 0.99):

$$c = 0.0035 - (2.42E-6)(t_{max} - t_{min})^2 \quad (14)$$

$$n = 2.17 + (1.83E-8)(t_{max} - t_{min})^{5.14} \quad (15)$$

Evaluating the Derived Function TF2

Values of TF2 calculated with the synthetic database were compared to results from $TF_{integrated}$ (fig. 6). The values are nearly identical (compare figs. 2 and 6). Values of TF2 for the 18 locations in table 1 agreed closely to values estimated with $TF_{integrated}$, as indicated by the small RMSE and CV and the large R^2 (table 2). When TF2 was compared to the two original methods of calculating TF, results were similar to those of comparing these two methods to $TF_{integrated}$. A close agreement between TF2 and $TF_{integrated}$ is apparent from the plot of TF values for the 18 locations (fig. 7).

Estimates of wheat residue decomposition using TF2 and the original TF method in RUSLE were compared for several locations in the U.S. The decomposition coefficient for wheat from RUSLE of –0.008 was used for estimating mass remaining over time. Published data from different environments can be difficult to use for this type of comparison because of variations in collection techniques, residue quality, and management practices (Christensen, 1986; Stott et al., 1990; Stroo et al., 1989; Douglas and Rickman, 1992). However, results of the evaluation indicate a small improvement in prediction accuracy with the TF2 approach. Plots of measured versus estimated mass remaining are presented in fig. 8. A paired t–test of the means and an F ratio of the variances (comparing observed to predicted) indicated closer agreement to the observed data with the TF2 approach (data not shown). For both TF and TF2, the predicted population means and variances were significantly greater than those of the observed data. Regression of TF and TF2 predicted values vs. observed values indicated a more negative intercept (–26.9 vs. –12.7) and greater slope (1.17 vs. 1.02) for the TF approach compared to the TF2 approach (fig. 8). Trends away from a one–to–one line could be influenced by other components used in the estimation of mass remaining (i.e., the water function and decomposition coefficient for wheat), as well as errors in the actual measurements.

The chi–squared value for goodness of fit indicated significantly different populations for TF2 and TF compared to the measured data, but the chi–squared value for TF2 was numerically smaller than that for TF (274 vs. 482, respectively). An estimate of agreement between predicted and observed data was determined from the chi–squared accuracy approach of Freese (1960). A non–significant chi–squared value (indicating similar populations) is obtained when the acceptable accuracy was set at ±32% mass remaining for TF and ±25% mass remaining for TF2, indicating improved predictions with TF2. Decomposition coefficients (K values) were fit to the field data with both approaches to determine how much different these data might be from the data used in developing the original decomposition coefficient in RUSLE. The new values were –0.0041 and –0.0048 for TF and TF2, respectively. These values are nearly half of the currently used value of –0.008 and indicate the variability present in field data originating from different climates and residue resources. The TF2 function appears to be an

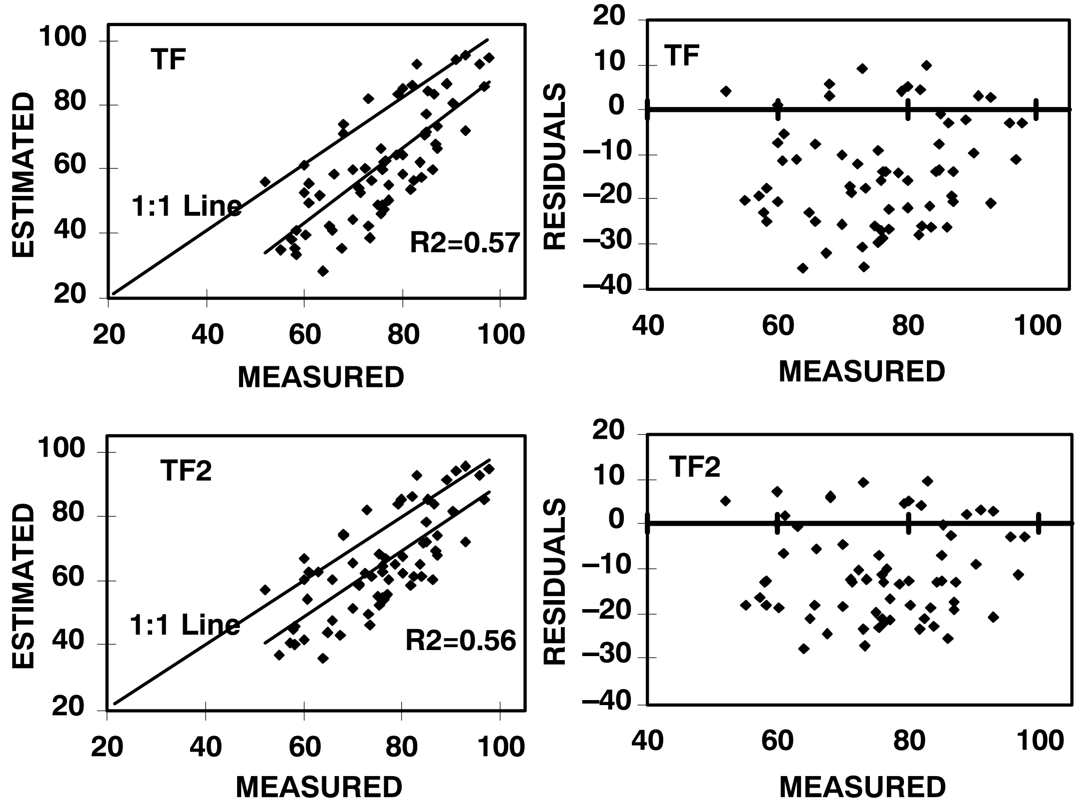

Figure 8. Measured versus estimated mass remaining (%) for wheat residue estimated with RUSLE using the original TF and newly developed TF2. Residual plots are for the same data, indicating the difference between measured and estimated values.

improvement over the original TF used in RUSLE, based on the closer agreement between measured and predicted mass remaining for the field data.

Summary and Conclusions

Our analysis indicated that the current approach of using monthly average or maximum and minimum temperatures does not capture temperature dynamics because of the averaging process and could be improved with a more numerically based function. A system of equations was developed that produces results similar to integrating the temperature from maximum to minimum using monthly data but requiring less computation time than the integrated method. The results are also similar to those estimated with an integrated function using daily data. The new approach (TF2) provides a better estimate of temperature effects on residue decomposition for long time steps like those used in RUSLE and RWEQ. The system of equations could be used to improve decomposition estimates in other monthly time step models and could be applicable in daily time step models. Our approach to developing the equations could be used to develop similar relationships for temperature or other effects in biological process models.

Acknowledgements

A portion of this work was completed while the first author was working at the USDA–ARS Conservation Production Research Laboratory, Bushland, Texas. Support of the Dryland Cropping Systems Management Unit is gratefully recognized.

References

Aber, J. D., and J. M. Melillo. 1982. Nitrogen immobilization in decaying hardwood leaf litter as a function of initial nitrogen and lignin content. *Can. J. Bot.* 60(11): 2263–2269.

Brown, P. L., and D. D. Dickey. 1970. Losses of wheat straw residue under simulated field conditions. *Soil Sci. Soc. Am. Proc.* 34(1): 118–121.

Christensen, B. T. 1986. Barley straw decomposition under field conditions: Effect of placement and initial N content on weight loss and nitrogen dynamics. *Soil Biol. Biochem.* 18(5): 523–529.

Douglas, C. L., and R. W. Rickman. 1992. Estimating crop residue decomposition from air temperature, initial N content, and residue placement. *Soil Sci. Soc. Am. J.* 56(1): 272–278.

Douglas, C. L., Jr., R. R. Allmaras, P. E. Rasmussen, R. E. Ramig, and N. C. Roager, Jr. 1980. Wheat straw composition and placement effects on decomposition in dryland agriculture of the Pacific Northwest. *Soil Sci. Soc. Am. J.* 44(4): 833–837.

Ford, P. B. 1991. Crop residue management as an integral component of sustainable crop production. MS thesis. Athens, Ga.: University of Georgia.

Foster, G. R. 1991. Advances in wind and water erosion prediction. *J. Soil Water Conserv.* 46(1): 27–29.

Freese, F. 1960. Testing accuracy. *Forest. Sci.* 6(2): 139–145.

Fryrear, D. W., J. D. Bilbro, A. Saleh, H. Schomberg, J. E. Stout, and T. M. Zobeck. 2000. RWEQ: Improved wind erosion technology. *J. Soil Water Conserv.* 55(2): 183–189.

Lischke, H., T. J. Löffler, and A. Fischlin. 1997. Calculating temperature dependence over long time periods: Derivation of methods. *Ecol. Model*. 98(2–3): 105–122.

Meentemeyer, V. 1978. Macroclimate and lignin control of litter decomposition rates. *Ecology* 59(3): 465–472.

Nicks, A. D., L. J. Lane, and G. A. Gander. 1995. Weather generator. In *USDA Water Erosion Prediction Project (WEPP): Hillslope Profile and Watershed Model Documentation*, 2.1–2.22. D. C. Flanagan and M. A. Nearing, eds. NSERL Report No. 10. West Lafayette Ind.: National Soil Erosion Research Laboratory.

Parr, J. F., and R. I. Papendick. 1978. Factors affecting the decomposition of crop residues by microorganisms. In *Crop Residue Management Systems*, 101–129. W. Oschwald, ed. Madison, Wisc.: ASA.

Reinertsen, S. A., L. F. Elliott, V. L. Cochran, and G. S. Campbell. 1984. Role of available carbon and nitrogen in determining the rate of wheat straw decomposition. *Soil Biol. Biochem.* 16(5): 459–464.

Roper, M. M. 1985. Straw decomposition and nitrogenase activity (C_2H_2 reduction): Effects of soil moisture and temperature. *Soil Biol. Biochem.* 17(1): 65–71.

SAS. 1988. *SAS/ETS User's Guide*. Version 6, 1st ed. Cary, N.C.: SAS Institute, Inc.

_____. 1989. *SAS/STAT User's Guide: Volume 2*. Version 6, 4th ed. Cary, N.C.: SAS Institute, Inc.

Schomberg, H. H., and J. L. Steiner. 1997. Comparison of residue decomposition models used in erosion prediction. *Agron. J.* 89(6): 911–919.

Schomberg, H. H., J. L. Steiner, and P. W. Unger. 1994. Decomposition and nitrogen dynamics of crop residues: Residue quality and water effects. *Soil Sci. Soc. Am. J*. 58(2): 372–381.

Steiner, J. L., H. H. Schomberg, C. L. Douglas, Jr., and A. L. Black. 1994. Standing stem persistence in no–tillage small–grain fields. *Agron. J*. 86(1): 76–81.

Steiner, J. L., H. H. Schomberg, and P. W. Unger. 1995. Residue decomposition submodel. In *Wind Erosion Prediction System Technical Description*, D1–D9. Initial version released at the symposium *WEPP/WEPS: The New Generation of Water and Wind Erosion Technology*. 9–11 August. Des Moines, Iowa: Soil and Water Conservation Society.

Stott, D. E., L. F. Elliott, R. I. Papendick, and G. S. Campbell. 1986. Low temperature or low water effects on microbial decomposition of wheat residue. *Soil Biol. Biochem*. 18(6): 577–582.

Stott, D. E., H. F. Stroo, L. F. Elliott, R. I. Papendick, and P. W. Unger. 1990. Wheat residue loss from fields under no–till management. *Soil Sci. Soc. Am. J*. 54(1): 92–98.

Stott, D. E., E. E. Alberts, and M. A. Weltz. 1995. Plant residue decomposition and management. In *USDA Water Erosion Prediction Project (WEPP): Hillslope Profile and Watershed Model Documentation*, 9.1–9.16. D. C. Flanagan and M. A. Nearing, eds. NSERL Report No. 11. West Lafayette Ind.: National Soil Erosion Research Laboratory. Available at: http://topsoil.nserl.purdue.edu/NSERLWeb/weppmain/weppdocs.html.

Stroo, H. F., K. L. Bristow, L. F. Elliott, R. I. Papendick, and G. S. Campbell. 1989. Predicting rates of wheat residue decomposition. *Soil Sci. Soc. Am. J*. 53(1): 91–99.

USDA. 1996. *Predicting Soil Erosion by Water: A Guide to Conservation Planning with the Revised Universal Soil Loss Equation. (RUSLE)*. USDA–Agricultural Handbook No. 703. K. G. Renard, G. R. Foster, G. A. Weesies, D. K. McCool, and D. C. Yoder, coordinators. Washington, D.C.: USDA.

USDA–ARS. 2001. CLIGEN Weather Generator, expanded and improved by USDA Agricultural Research Service and U.S. Forest Service. West Lafayette Ind.: National Soil Erosion Research Laboratory. Available at: http://horizon.nserl.purdue.edu/cligen.